DFG-Reference: GS 14/1-2

November 2002

Dr Michael Gschwendtner
Department of Mechanical Engineering
University of Canterbury
Christchurch
NEW ZEALAND

FINAL REPORT

on

"Experimental Investigation of Regenerator Materials in Stirling-cycle Machines"

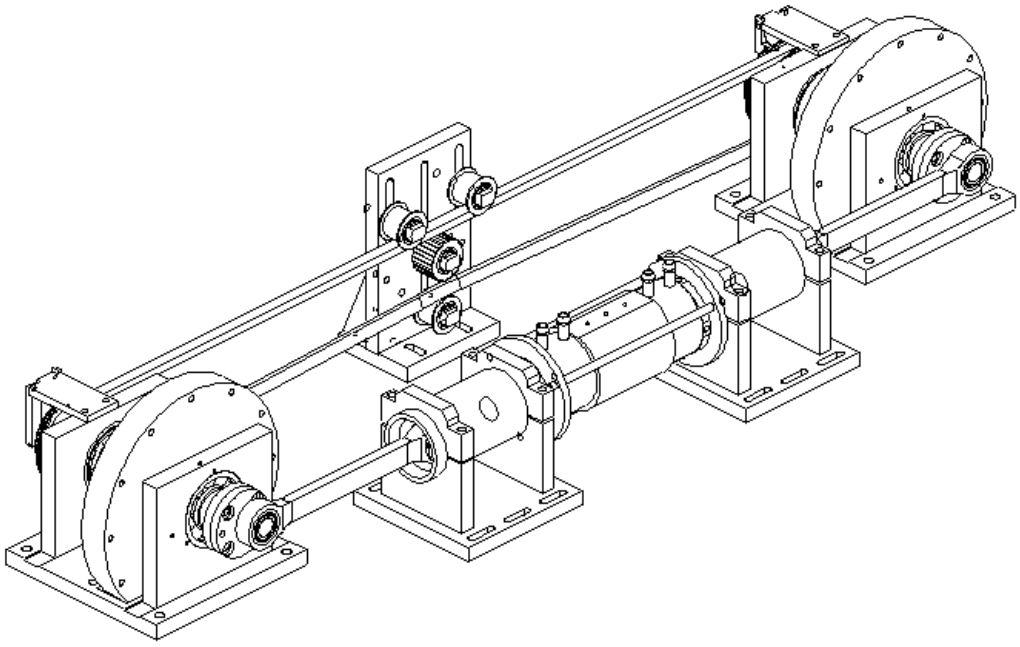

Contents

1. Introduction

In Stirling cycle machinery, the regenerator plays a key role in determining overall efficiency of the system. The regenerator acts to provide internal temporary storage of heat which would otherwise have to be added to the system from outside.

In general, the regenerator comprises a porous material (usually a metallic mesh) through which the working gas flows periodically. Coming from the hot end, the gas rejects heat while passing the colder regenerator matrix; the heat is temporarily stored in the wire mesh until it is released to the working fluid coming back from the cold end. The Stirling Cycle is characterised by two isochoric and two isothermal processes. In the ideal case, heat exchange with the surroundings occurs only during the isothermal expansion and compression phases. Since the temperature of the working gas has to be changed during the isochoric phases (by means of the internally stored energy), the theoretical Carnot-efficiency can only be reached with a regenerator.

Despite the regenerator's simple function (i.e. storing heat from the working gas during one part of the cycle and releasing it during another) the actual process is very complex and not yet completely understood. In practice, two effects seem to mutually exclude each other. On one hand, high gas velocities in the regenerator are desirable in order to achieve a good heat transfer; on the other hand, the higher velocities also lead to greater flow losses across the regenerator matrix. Thus, in designing a regenerator configuration it seems as if one has the choice of either good thermal behaviour or low friction losses, but not both. Furthermore, the same solution for this problem cannot be expected to be applicable to all types of Stirling-cycle machine. The ideal configuration will vary from application to application and will be dependent on parameters like size, speed, temperature, geometry, materials, etc. However, thorough experimental investigations and theoretical analysis will contribute to a better understanding of the processes in a regenerator, and will therefore help to improve the efficiency and to determine the appropriate configuration for each application.

2. Project description

The aim of this project is to design a test-rig to be able to systematically investigate various matrix materials with different geometries in order to determine dependence of cycle speed, volume ratios, gas pressure, etc. Emphasis has been laid on a basic experiment which produces results in a general form applicable to different types of Stirling-cycle configuration. The purpose of this project was not to design a competitive regenerator configuration, but rather to provide general test conditions to investigate the influence of various parameters.

Figure 1 shows the main parameters of regenerator configuration. The matrix is usually placed in an annular gap through which the working gas flows periodically. In order to provide a smooth transition for the flow path a filler is placed in between.

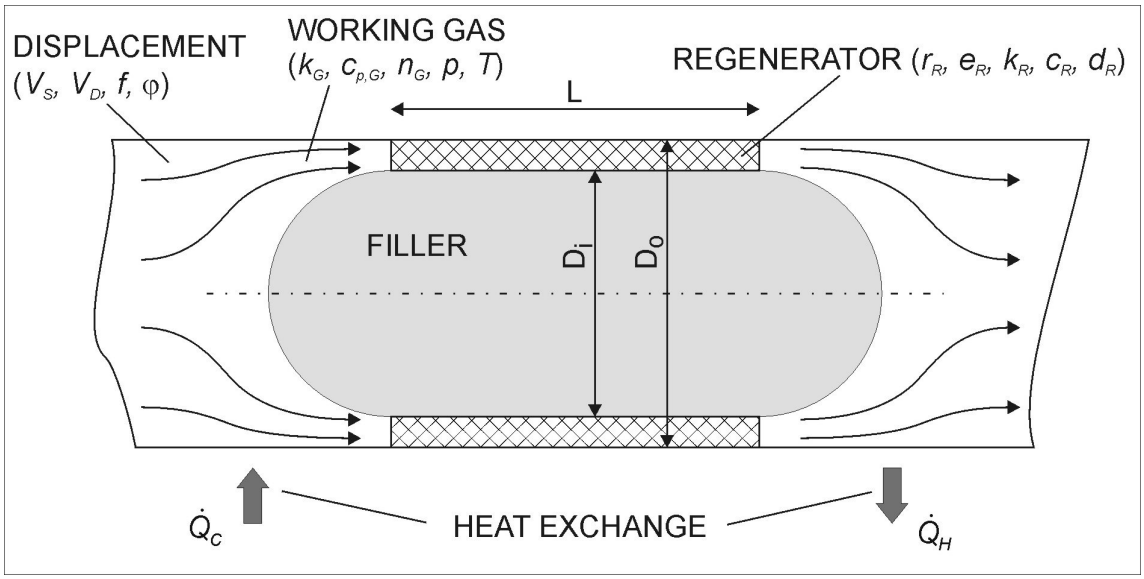

Figure 1: Regenerator parameters

The fundamental regenerator set-up can be described by the length L and the inner and outer diameters D_i and D_o. The relevant regenerator properties are the material density ρ_R, the heat conductivity k_R, the specific heat capacity c_R, the fibre/wire diameter d_R and the porosity ε_R (defined as the ratio of gas volume in the regenerator to the overall regenerator volume):

$$\varepsilon_R = \frac{V - V_{MATRIX}}{V}.$$

The working gas is characterized by its heat conductivity k_G, the specific isobaric heat capacity $c_{p,G}$, the kinematic viscosity ν_G, the pressure p, and the temperature T.

The displacement parameters are the swept volume V_S, the dead volume V_D, the frequency f, and the phase angle φ between the two pistons. The description of the experiment is completed by the absorbed and rejected heat $\dot{Q}_C$ and $\dot{Q}_H$ respectively.

Apart from these parameters, the following dimensionless numbers are introduced:

- Reynolds number: $Re = \frac{dv}{\nu} = \frac{(D_o - D_i)v}{\nu}$

As a dimensionless velocity, the Reynolds number represents the ratio of inertia to viscosity and is related to a characteristic length d. For an annular gap the characteristic length is the hydraulic diameter d_h, which is twice the gap width (in this

case $d_h = (D_o - D_i)$). Note, that the porosity ε_R cancels out as it both reduces the hydraulic diameter and increases the free flow velocity v_∞ at the same rate.

- Fanning friction factor: $$F_f = \frac{\Delta p d_h}{2 \rho v^2 L}$$

The Fanning friction factor takes account for the friction loss in a piping system. It represents the ratio of shear stress at the wall to the kinetic energy of the flow, with ρ being the density of the fluid, v the velocity averaged over a section of pipe, Δp the pressure drop, d_h the hydraulic diameter and L the length of the pipe.

3. Literature

Experimental work on flow friction and heat transfer characteristics of various types of regenerator materials in an oscillating flow has been performed by Tanaka and Chisaka (1988). They found the following empirical relation between the friction factor f_h and the Reynolds number Re_h which contains the hydraulic diameter as the characteristic length, formed of porosity, mesh diameter and mesh shape:

$$f_h = \frac{175}{Re_h} + 1.60 .$$

Comparisons with steady flow experiments showed a higher pressure loss in oscillating flows at a given Reynolds number. The heat transfer coefficient was found by measuring the fluctuating gas temperature at the ends of the regenerator. In contrast to an ideal regenerator, temperatures do not remain constant in a real regenerator but vary periodically due to the limited heat transfer coefficient and surface area. The heat transfer loss of the regenerator was estimated from its geometry and the heat transfer coefficient. Measuring the rejected heat from the cooler as a comparison verified the accuracy of the obtained results. Experiments showed that the mean heat transfer coefficient increases with increasing mesh number and mean velocity. For the wire netting the following equation was obtained for the Nusselt number Nu_h and the Reynolds number Re_h:

$$Nu_h = 0.33 \quad Re_h^{0.67}$$

The heat transfer of the sponge metal seemed to be lower than that of the wire-netting for a given Reynolds number. Also, the diameter of the wire-netting has a strong impact on the ideal length of the regenerator. With very thin diameter wire-netting the length of the regenerator should be shorter to avoid a large pressure loss. However, with very thick diameter wire-netting, the length of the regenerator should not be too short due to the low heat transfer coefficient.

Tsuchiya et al. (1988) proposed a new measuring method for the pressure loss in a regenerator matrix under periodic flow. The tube containing the regenerator material was connected to a chamber, and the periodic flow was generated by an adjustable sinusoidal wave oscillator and a speaker. By measuring the oscillating pressure at the entry and the exit of the statements on the friction factor of the matrix then were derived.

Hamaguchi et al. (1988) carried out tests with regenerator matrices composed of different mesh properties. The decision on the optimum combination was made by looking at the time averaged temperature profile along the regenerator. In comparison to single mesh matrices, combined mesh matrices showed a smaller flow loss with the largest temperature drop at the hot end of the regenerator due to the smaller velocities inside the regenerator. The authors found the best combination for their engine to be a stack of coarse mesh gauzes at the cooler side, with a stack of fine mesh gauzes at the hot side.

In a more recent paper Hamaguchi et al. (1993) carried out tests with different mesh combinations in a free-piston Stirling engine and confirmed a superior regenerator behaviour in contrast to single mesh types.

A theoretical design study of regenerators was performed by Isshiki and Watanabe (1988). In modelling the process for an α-type Stirling engine, they came to the conclusion that the total dead volume and the dead volume in the regenerator mesh have a big influence on the total efficiency.

In order to increase the overall efficiency of a double acting Stirling engine Kojiama et al. (1988) constructed a test rig to perform numerous test with various regenerator elements. However, pressure loss was investigated under steady flow conditions. The authors found linear tube type regenerators to be effective in reducing flow losses, but wire mesh types showed a better heat transfer coefficient.

In their parametric analysis on regnerator efficiency Bartolini and Pelagalli (1991) confirmed that the thermal efficiency increases with smaller pitches between the wires of the mesh as a consequence of better heat transfer. However, the wire diameter itself had a smaller influence on the thermal efficiency at larger pitches. For given pitch distances two contradictory effects take place with increased wire diameter. The larger heat transfer area is offset by a shorter time taken for the gas to cross the matrix. Furthermore, a lower speed of revolution and a smaller pitch in the flow direction both increased the thermal efficiency and diminished the influence of the pitch normal to the flow direction. In the case of a ball matrix, the authors came to the conclusion that both a smaller ball diameter and a reduced speed increased the thermal efficiency. As the authors point out, a difference in the behavior of all geometric parameters obviously occurs when either the regenerator mass or the regenerator volume are regarded to be constant. At any rate, a large surface area is responsible for the thermal efficiency of the regenerator. It should be noted however, that no pressure loss in the regenerator was accounted for in this analysis.

Moriya et al. (1991) report about experiments on temperature efficiency and flow resistance of heat regenerator materials in an internal combustion Stirling engine. Stainless steel wire mesh, stainless steel wool, stuffed wire mesh, compressed foam metals, Helipack, ceramic ball, ceramic pipe and twisted wires were tested. The authors point out that the stuffed wire mesh appeared to be most favorable in respect to both flow loss and thermal efficiency.

Tsuchiya et al. (1991) classified regenerator materials into two major groups in terms of flow path. One group can be characterised by a complicated and random flow path, the other group by a straight and simple flow path. The authors suggest a

division of the occuring pressure loss into one caused by inertia of the fluid in the matrix and described by the Euler number, and one caused by the fluid viscosity, which can be described by the Fanning friction number. Two empirical formulas are given for both groups of regenerator materials from which the pressure drop from periodic flow can be evaluated.

In more recent work Tsuchiya et al. (1993) found out that the resistance of a straight pipe under periodic flow is nearly 1.6 times larger than under steady flow. Furthermore, curved pipes only slightly increase the flow resistance. The results of an increased number of pipes would therefore suggest that the given formula for a single pipe is applicable to heat exchanger components comprised of many pipes, since the flow characteristics remain the same. The authors also found out that the majority of pressure drops across heater and cooler pipes is induced by inertia effects, whereas those across the regenerator matrix are mainly due to viscous effects.

Analytical work on thermo-fluids of a regenerator was done by Kentfield (1993). He shows that the energy quantity removed from and returned to the working fluid in a Stirling engine type regenerator is γ times the corresponding internal energy difference (where γ is the working fluid specific heat ratio). Since the flow work of the hot gas leaving the regenerator is higher than the flow work of the cold gas entering the regenerator, the difference increases the effective energy storage within the regenerator matrix.

Carlsen et al. (1993) varied the length of a stainless steel regenerator mesh in a Vuilleumier heat pump driven by a gas burner. Due to the increased length of the regenerator the pressure drop in the hot section was higher and thus the speed of the heat pump dropped. On the other hand, the COP increased significantly. As their results show, there is no further increase of the COP with an increased input heat temperature after a maximum was reached, though the Carnot value increases. This indicates a high thermal loss in the hot section of the heat pump. A computer simulation program was in good agreement with their experimental results.

Tanaka (1993) investigated the effects of wire diameter, regenerator shape, engine speed and gas pressure on the regenerator performance in an oscillating flow. Considering the significant temperature dependence of gas properties (such as viscosity and density), Tanaka discovered a higher indicated thermal efficiency when thick wire was installed to the hot side of the regenerator (in direct contrast to Hamaguchi et al. (1988)!). A further result of his investigation was that thin wire is better suited for regenerator matrices with a shorter length, whereas thick wire is suitable for a long length regenerator. Furthermore, the thermal efficiency decreases with engine speed, but remains high with increased gas pressure.

An analytical solution for the effectiveness of regenerators in β-type Stirling engines is given by Benvenuto and De Monte (1995). The comparison with the performance data of a single cylinder free-piston Stirling engine shows a 5 % higher effectiveness for the assumed ideal case in the model.

Zhiyuan and Hongshuo (1995) carried out experimental investigations on different types of stainless steel wool with respect to thermal efficiency and flow resistance.

They discovered that there is not much difference in the regenerator behaviour in a Stirling engine running on normal conditions between a stainless steel wool and a stainless steel wire mesh. The authors therefore see the wool as a cost-effective substitute for the expensive wire mesh.

Tanaka and Hamaguchi (1995) investigated the influences of thermal performance of the regenerator, wire diameter size, and total dead volume, on the indicated thermal efficiency of a Stirling engine. Their results show that the indicated thermal efficiency has an optimum for wire diameter size. This is because the smaller the wire diameter, the better the heat transfer due to an increased surface area, but the higher is the pressure loss in the regenerator matrix. Furthermore, an increased dead volume reduces the engine power, and the efficiency is additionally more sensitive to wire diameter size.

Experimental work on combinations of different regenerator materials has been carried out by Lee and Kang (1997). The average porosity of the different stainless steel meshes was kept at a constant value of 0.7. Both the pressure loss and thermal efficiency were measured for different mesh types. The authors found the heterogeneous combination of fine wire mesh at the cold side of the regenerator and thick wire mesh at the hot side to be most effective in terms of pressure loss and regenerator efficiency. The reason for this is related to the density of the working gas, which is strongly dependant on temperature. As temperature increases and density reduces, the heat capacity per unit volume of the working gas also becomes lower. All different types of mesh combinations showed a decrease in efficiency with increased speed, however, the above mentioned combination still was better by around 5%.

In an analytical investigation Cho et al. (1997) discuss the effects of frequency and amplitude of the flow oscillations on regenerator effectiveness. They introduce the parameters $\beta = R\sqrt{\frac{\omega}{\alpha}}$ and $\lambda_s = \frac{L_s}{L_g}$ to describe these effects. The former represents the modified Womersley number which is interpreted to be the ratio of the hydraulic radius to the thickness of the Stokes thermal boundary layer. As their results show, the conventional definition of regenerator effectiveness is only valid for small frequencies, since the axial heat flow, which is not considered in this definition, increases with the speed. However, normal Stirling engine frequencies are still below this range.

Kühl and Schulz (1996) report about a 2nd order model which includes flow dispersion and bypass losses in a regenerator. At the beginning they discuss various losses in regenerators, whereas in each case other losses are neglected as it is usually the case in 2nd order approaches. As far as the reheat loss is concerned, the authors point out that an initial temperature difference between the gas and the regenerator matrix declines at a very high rate and is negligible after 5 - 10% of the regenerator length. The temperature swing loss, which is caused by the limited heat capacity of the matrix, seems to be overestimated according to Kühl and Schulz, since the assumed linear temperature profile along the regenerator differs from reality, particularly at the ends of the matrix.

In order to describe the loss due to dispersion within a porous flow system, the authors suggest a model employing a dispersion coefficient which is similar to chemical reactor theory. A physical explanation for this loss is given by a microscopic mixing of gas particles of different temperature within the pores of the matrix. Since mixing increases entropy, in an adiabatic regenerator this entropy can only be conveyed out by a flow of enthalpy from the hot to the cold end of the regenerator, i.e. a heat loss.

As a further result of their analytical model, it is concluded that bypass losses of pores and flow channels within the matrix are usually small, since they normally only exist over a short distance. As for the loss in the gap between the matrix and the regenerator wall, within a gap width of half the hydraulic diameter of the matrix this loss seems to be negligible.

Based on the results of former experiments on flow friction and heat transfer characteristics in randomly compressed wire regenerator materials, Kühl et al. (1998) suggest semi-empirical correlations eliminating the influence of the porosity. In contrast to the former correlations using the hydraulic radius, the authors suggest a different approach based on model assumptions concerning the characteristic length, the flow path and the actual heat exchange surface within the mesh.

Due to an increased flow path in a porous matrix, an elongation factor is introduced for the modified friction factor as well as for the Reynolds number. However, in contrast to the flow losses, a decreased surface area is assumed for the heat transfer due to the boundary layer around the wire.

As a summary, the following conclusions for the regenerator behaviour can be drawn from the investigations mentioned above:

- The higher the mesh number, the thinner the wire and the higher the porosity of the matrix is, the better is the thermal efficiency due to an increased surface area. However, the higher is the pressure loss.
- In contrast to steady flow, oscillating flow causes a higher pressure loss and a lower thermal performance at a given Reynolds number.
- With an increased mean velocity the heat transfer and also the pressure loss increase.
- The larger the heat transfer area, the shorter is the time taken by the gas to cross the matrix due to an increased velocity.
- Since the flow work of the hot gas leaving the regenerator is higher than of the cold gas entering the regenerator, the effective energy storage in the matrix is increased by this difference.
- Thick wire being installed at the hot end of the regenerator, and thin wire at the cold end respectively increases the indicated thermal efficiency (in contrast to Hamaguchi et al. (1988)). The heat capacity of the gas per unit volume, which strongly depends on the temperature, is thought to be the reason for this.

4. Experimental set-up

In order to keep as close to reality as possible, the experiments will be carried out (as opposed to many other investigations) in a periodic flow at typical Stirling engine speeds. Figure 2 shows the basic concept of the experiment.

In a single-cycle α-configuration, the arrangement of two opposing pistons provides an oscillating flow through both heat exchangers and the regenerator. The pistons are driven by an electric 2 kW-motor with adjustable speed up to 1000 rev/min. The crank mechanism allows the setting of various phase angles and is connected to the motor by a timing belt. In order to take advantage of the piston force during the expansion phase, flywheels are mounted on each crank shaft to store kinetic energy.

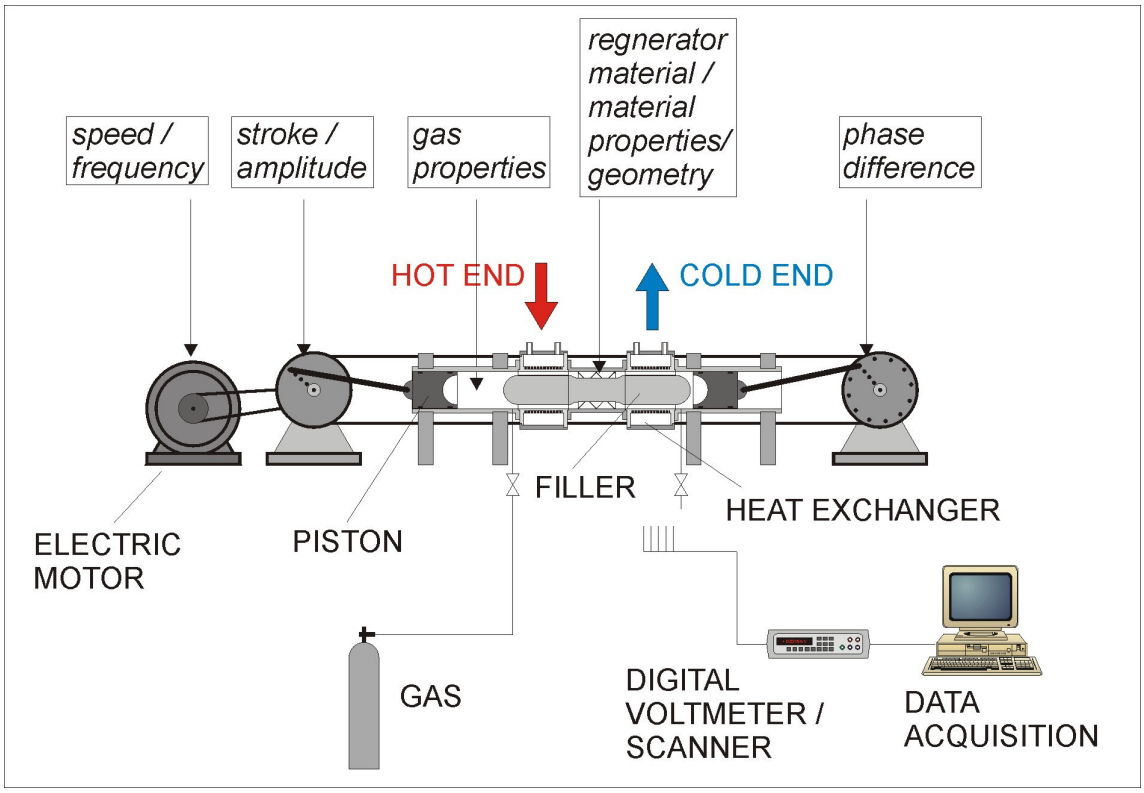

Figure 2: Experimental set-up

Different settings for the con-rods on the crank wheels allow variation of the piston strokes and thus the swept volume. Furthermore, the dead volume can be changed by altering the distance between the piston and the crank pin. Cylinders, heat exchangers and regenerator housing are sealed with o-rings and are clamped together by tie-rods. A maximum pressure of 35 bar can be realised, and two valves allow for top-up gassing to replace any leakage from the system. A variety of different

regenerator lengths can be tested in this rig and so all parts are mounted on blocks which can be aligned and fixed to a platform on the table.

The most relevant parameters of this experiment are the pressure loss across the regenerator, and the absorbed and rejected heat in the heat exchangers. Pressure transducers are mounted on each side of the regenerator housing in order to measure the pressure difference. The transducers are timed by a trigger system which is connected to the crank mechanism. An aqueous ethanol mixture flows through the heat exchangers and acts as a heatant or coolant respectively. By measuring the mass flow rate and the inlet and outlet temperatures the absorbed and rejected heat can be determined. Additional temperature transducers are placed within the regenerator to measure the temperature profile along the matrix. For all temperature measurements platinum resistance thermometers (PRTs) are employed. Finally, a data acquisition program collects all data and stores them in a file.

The test-rig is designed to operate over the temperature ranges typically found in heat-pumps and refrigerators. Due to a phase angle of 90° between the two pistons compression occurs on one side, and expansion on the other. Thus, heat is rejected in one heat exchanger and absorbed in the other. Since the amounts of heat are the critical parameters for the experiment, the following definition for an efficiency factor is suggested (Figure 3).

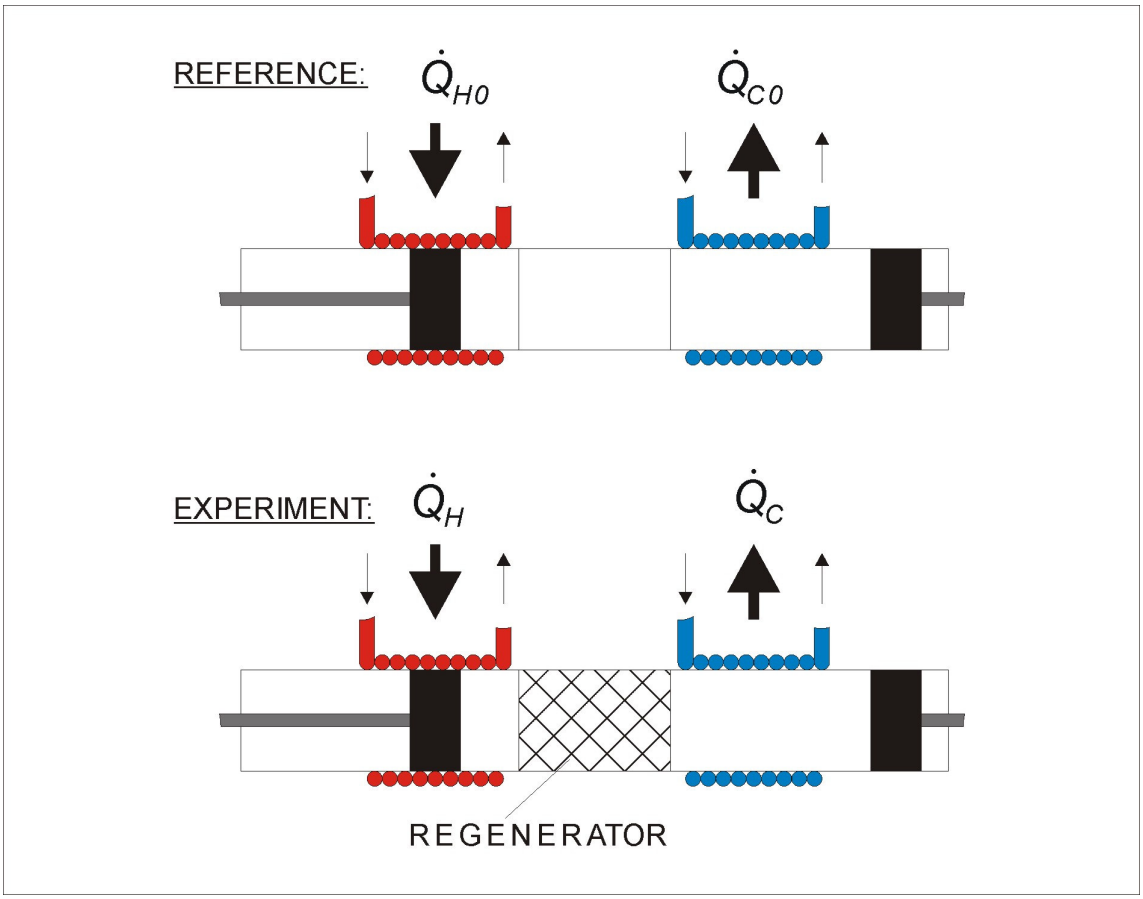

Figure 3: Definition of an efficiency factor

For each combination of parameters the absorbed and rejected heat are measured without a regenerator matrix as a reference. The following test series are then referred to this reference and an efficiency factor is defined as

$$\eta = \frac{\dot{Q}_{C0} - \dot{Q}_C}{\dot{Q}_{C0}} .$$

The advantage of this procedure is that all secondary influences are canceled out.

A similar procedure is possible to determine the flow losses in the regenerator matrix. In altering the phase angle to 0°, the working gas flows periodically and isochorically through the regenerator so that the friction loss is turned into heat. The heat is rejected on both heat exchangers and can be measured by the method described above. Thus, a measure is given for the friction loss of each regenerator material and configuration.

5. Components

For all parts of the experimental set-up fatigue calculations have been carried out. The test rig is designed for a maximum pressure of 35 bar and a speed of 1000 rpm. Also, the temperature range is that of typical heat-pumps and refrigerators.

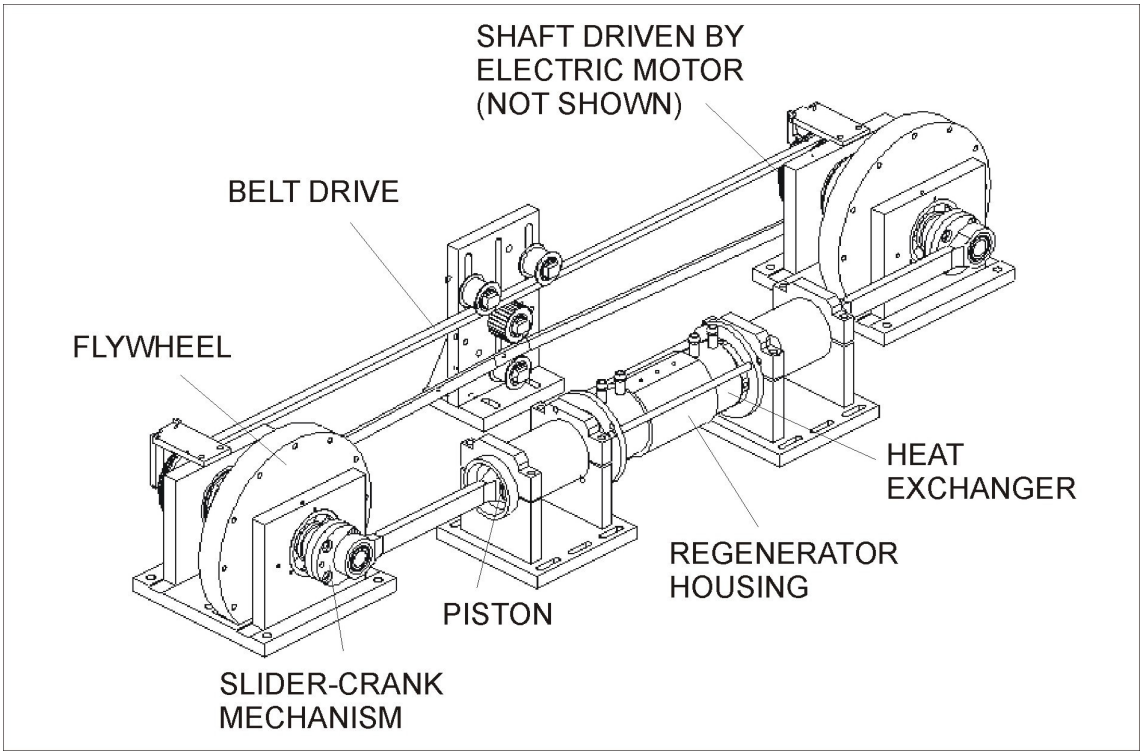

Figure 4: The main components of the test rig

In the following sections, only the most critical components of the test-rig are described. Figure 4 shows an assembly view of these parts.

All parts which contain the working gas are sealed with o-rings and are clamped together by three tie-rods. The regenerator housing in the middle is framed by two heat exchangers, which themselves are held in place by the cylinder liners. In order to allow thermal expansion, one cylinder liner can slide along the blocks on which it is mounted, while the other is in a fixed position to bear the axial forces of the pistons. Both cylinder liners are clamped to the mounting blocks which are bolted to a plate.

5.1 Heat exchangers

The starting point for the design of the test rig were the heat exchangers, which are the same as the ones used in an existing machine designed by the Stirling-cycle Research Group at Canterbury University (designated "DH1"). The reason for this is so that the results of the experiments are directly comparable to an existing machine of exactly the same dimensions but of a different type.

Figure 5 shows a cross-section of the DH1-heat exchanger. They are designed using the Stirling simulation program SAGE and incorporate 198 slots wire-cut in an axial direction on the inner side of the heat exchanger through which the working gas flows. The slots are 3 mm deep and 0.3 mm wide.

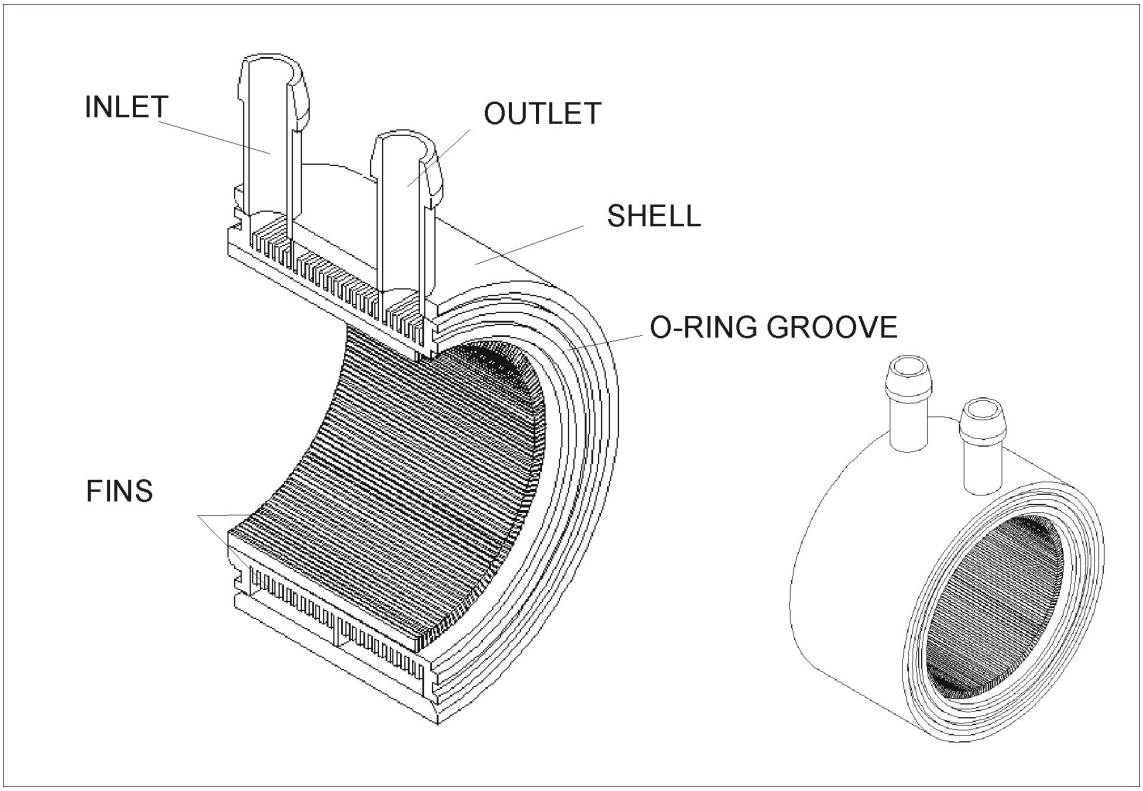

Figure 5: The DH1-heat exchanger in a section view

To improve the heat transfer to the heatant or coolant liquid, grooves are cut in circumferential direction on the outer side. These slots are 7 mm deep and 1 mm wide. A brass shell is soldered to the heat exchanger to close the circuit.

5.2 Regenerator

In order to test various geometries of regenerator matrices, housings of different lengths will be used. Figure 6 shows the assembly of the regenerator housing and the two heat exchangers. A body is placed in the centre to fill out the void space and to direct the gas flow through the fins. The filler end-pieces have a spherical shape for a smooth flow transition. In between both ends, segments of different diameters can be placed in order to vary the matrix geometry in width and length. All parts are screwed together by a tie-rod.

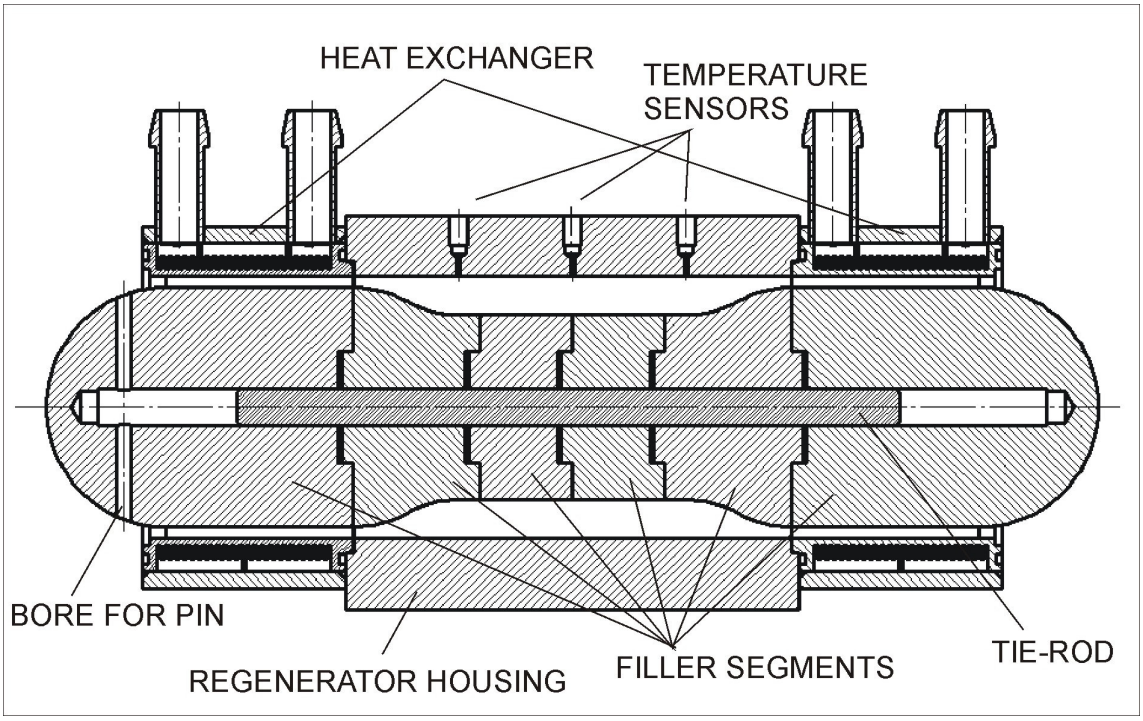

Figure 6: The regenerator assembly

The regenerator material will be placed in the space between the housing and the filler. Some combinations of filler segments produce a smooth flow transition (as shown in Figure 6) while others create a step, which necessitates wire mesh regenerator material to be wound around the inner filler segment. The following volumes can be achieved by altering the filler combinations, as shown in Table 1:

Table 1: Regenerator volumes with different filler combinations

FILLER	DIAMETER "A"	DIAMETER "B"	DIAMETER "C"
2 STRAIGHTS	49.99 cm^3	66.51 cm^3	95.64 cm^3
2 CURVED	-	59.88 cm^3	80.22 cm^3
2 STRAIGHTS + 1 SEGMENT	64.99 cm^3	86.44 cm^3	124.31 cm^3
2 CURVED + 1 SEGMENT	-	79.82 cm^3	108.89 cm^3
2 STRAIGHTS + 2 SEGMENTS	79.98 cm^3	106.38 cm^3	152.98 cm^3
2 CURVED + 2 SEGMENTS	-	99.75 cm^3	137.57 cm^3

Figure 7 illustrates possible combinations of filler segments to achieve approximately identical volumes at various regenerator lengths and widths.

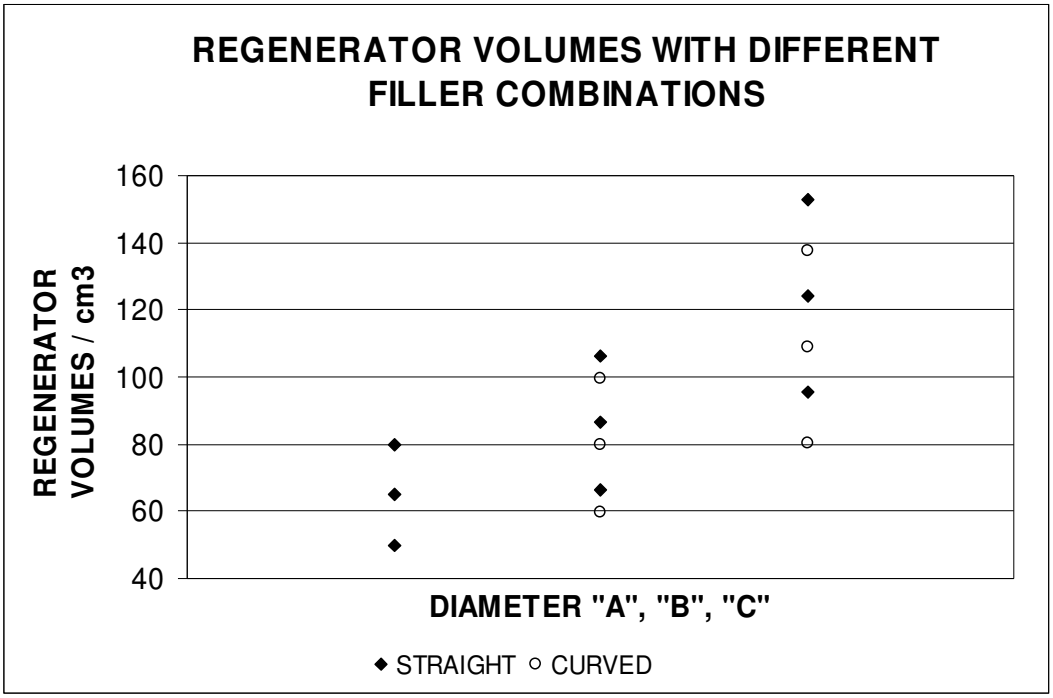

Figure 7: Achievable regenerator volumes with various filler segments

Since the filler offers resistance to the flow, the filler must be positioned in an axial direction. In order to carry this axial load, a bolt (not shown in Figure 6) passes through the end of the cylinder liner and one end of the filler. Both the housing and the filler are made of plastics - Ertacetal H - which is strong enough to bear the maximum pressure of 35 bar and is a good insulator at the same time. The heat flow both in the axial direction and to the surroundings has to be minimized. At the top of

the regenerator housing are three narrow holes allowing platinum resistance thermometers to be fitted, and thus the temperature profile measured in an axial direction.

5.3 Pistons

As well as the regenerator housing and the filler, both pistons are also made of plastics. Ertacetal H is both capable of withstanding high mechanical stresses and can also tolerate temperatures up to 150 °C. Further advantages are that this material can be easily machined, and is of low density.

In Figure 8, both a sectional and an isometric view of the piston are shown. The piston end has a spherical hollow which is slightly bigger than the filler end. This is to minimize the dead volume. Grooves for guide rings and seal rings are cut in the outer surface of the piston.

The part which is connected to the con-rod (not shown in Figure 8) is made of steel and can be screwed into the piston. The recess for centering is deep enough to provide room for different spacer rings. With these spacer rings the distance between the crank pin and the gudgeon pin can be altered, and thus various quantities of dead volume can be set. The piston stroke, and thus the swept volume can be varied by different crank radii (see 5.4).

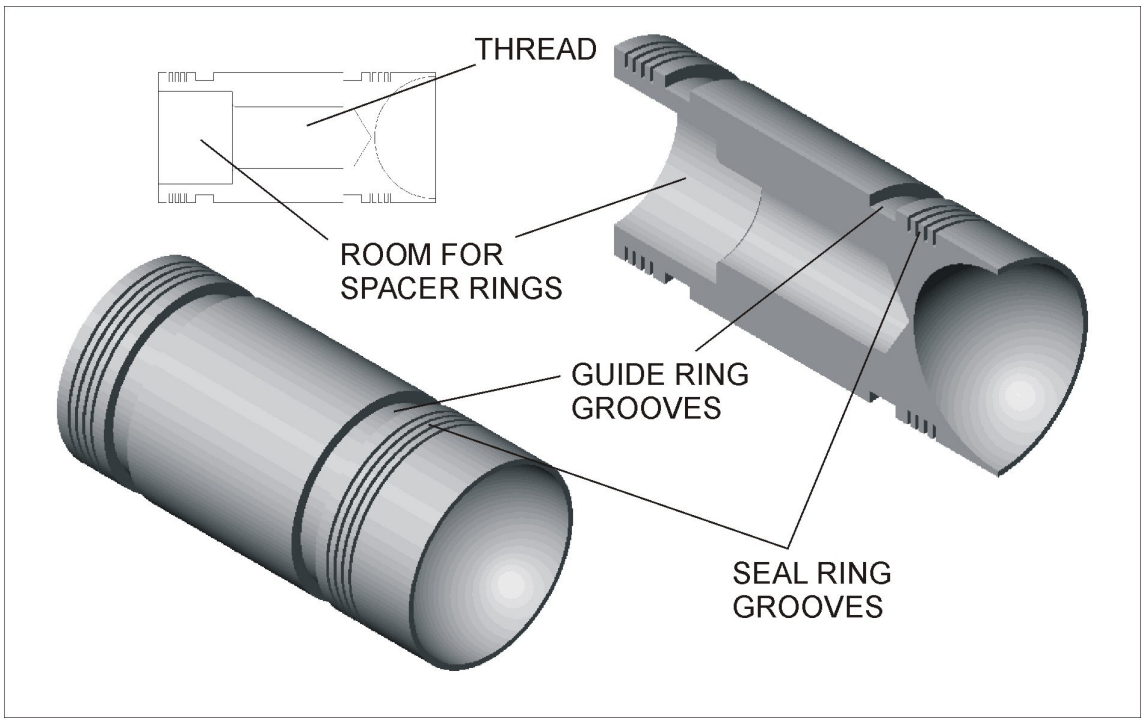

Figure 8: Different views of the piston

Particular attention was paid to the seals as they have a critical influence on the performance of any Stirling cycle machinery. It is a key part of the Stirling Cycle Research Group's programme to investigate the employment of low-cost rubbing seals in Stirling heat-pumps and refrigeration systems. Part of the results were presented at the *10th International Stirling Engine Conference 2001* in Osnabrück/Germany (Haywood, D., Raine, J.K., Gschwendtner M.A., 2001). The outcome of these investigations affected the decision on the number of rubbing seals in the design of the MAG1 regenerator test-rig.

Three main pathways have been identified for gas leaking through the piston pack:

- Wall gap - as the piston slides within the cylinder a certain amount of leakage occurs between the rubbing face of the seal and the cylinder wall.
- Ring gap - leakage takes place through the ring gap whenever there is a pressure difference across the piston.
- Pressure reversal - quite large amounts of leakage occur when the pressure across the piston is reversed. This causes the ring to jump from one side of the ring-groove to the other, momentarily producing a very significant leakage path and allowing a "puff" of gas to pass behind the seal.

A series of basic experiments using a range of piston seal configurations in the DH1 heat-pump were carried out in order to investigate the seal behaviour. As a result, for instance, the examination of the outer seal rings showed that they were more worn than the inner ones. This indicates that additional piston rings are less loaded and therefore do not contribute to a significant increase of friction losses. Additional rings also increase the flow resistance during the pressure reversal process, and thus reduce gas leakage. On the other hand, providing adequate sealing performance with a higher number of seals also leads to increased friction losses.

However, since mechanical efficiency plays a minor role for this test-rig the main focus was laid on good seal performance. Eight seal rings of low wear rate polymeric material were chosen for each piston, which delivers sufficient sealing to avoid the need for a pressurized crank case. Seal springs were placed in each seal spring groove (between the piston and the seal rings) to provide an adequate pre-load.

5.4 Slider-crank mechanism

The flow through the regenerator matrix is provided when the two opposing pistons are driven by the slider-crank mechanism. Since the test-rig is designed to allow direct comparisons with the DH1heat-pump due to identical heat exchanger design, the piston bore was therefore set at 71 mm. Assuming similar values of swept volumes to the DH1 heat-pump, the crank radius could be determined. In order to vary ratios of swept volume to dead volume or regenerator volume, the piston stroke was made variable. The initial idea of an adjustable crank pin was rejected for design and manufacturing reasons. Instead, three sets of crank pins with fixed radii were manufactured. The chosen crank radii of 6.3, 10.1 and 13.9 mm provide swept volumes of 50 cm^3, 80 cm^3 and 110 cm^3, which is of the same order of magnitude as the achievable regenerator volumes and swept volume of the DH1 heat-pump.

Figure 9 illustrates the design of the slider-crank mechanism. Needle roller bearings support both the gudgeon pin and the crank pin in the con-rod. The crank pin sits on a disc which is eccentrically machined in one piece. This disc can be bolted to the end flange of the drive shaft by four bolts. A recess and a dowel ensure accurate position of the crank pin once it had been removed.

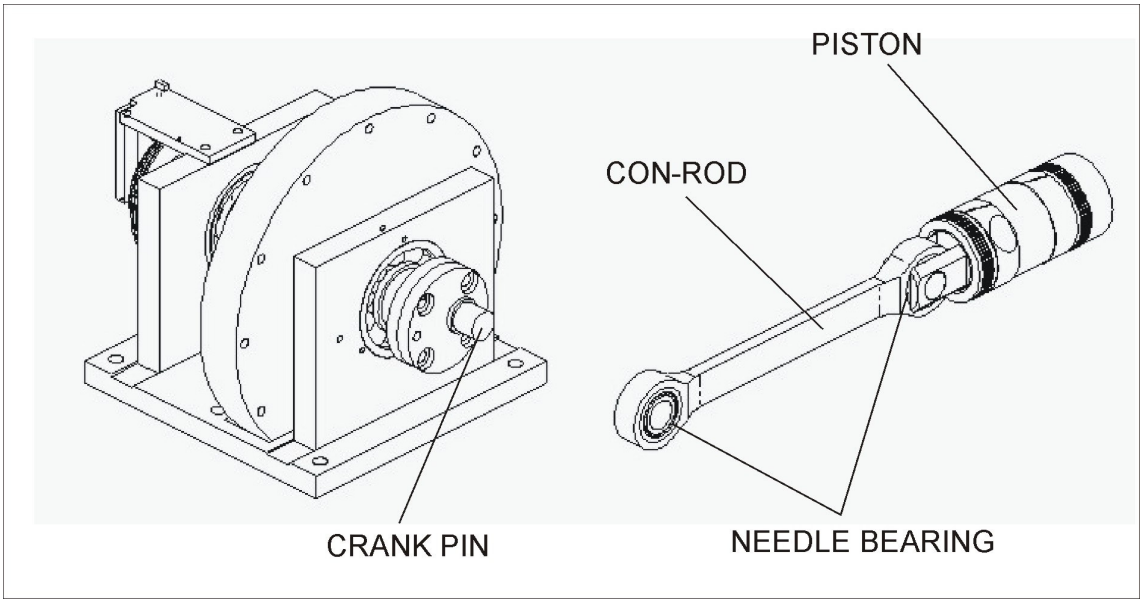

Figure 9: Slider-crank mechanism

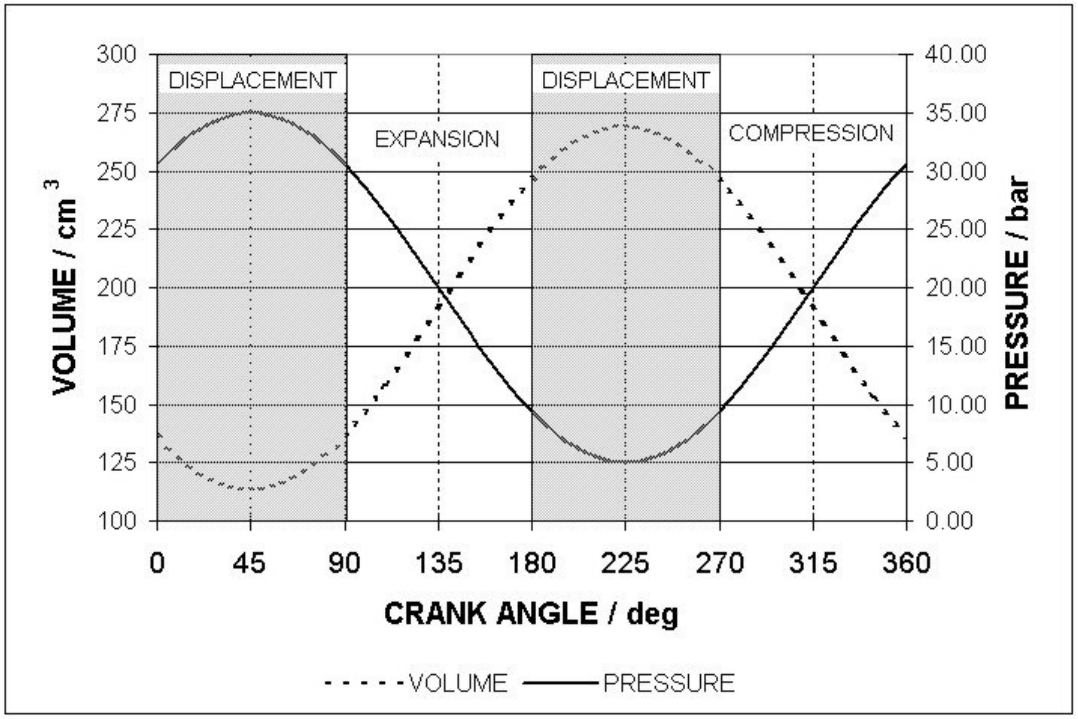

Figure 10: Regenerator volume and pressure over a complete cycle

A light push fit between the inner ring of the needle bearing and the crank pin facilitates the removal of the con-rod. A small disc centrally bolted on to the crank pin (not shown) locates the inner ring in the axial direction.

A phase angle of 90° between the two shafts creates the characteristic Stirling-cycle consisting of two isothermal and two isochoric processes. Figure 10 shows the functions of pressure and volume of the working gas with respect to the crank angle over a complete cycle. The data was calculated for the following configuration: regenerator volume 80 cm^3, crank radius 13.9 mm, mean gas pressure 20 bar.

5.5 Flywheel

The large cylinder diameter of 71 mm, and a maximum gas pressure of 35 bar, result in relatively high piston forces of about 14 kN. With the two shafts connected to each other via a belt drive, this requires a maximum torque for the electric motor of ± 180 Nm. The average torque over the complete cycle, however, is only 2.3 Nm for the given configuration. In order to smooth out the high reciprocating piston forces and to take advantage of the compression energy stored in the working gas, flywheels were mounted on each shaft. Depending on the stroke, the mean piston work can then be calculated to 220 J, the amount of energy which should be stored in form of rotational kinetic energy in the flywheel. In order to obtain the required moment of inertia of the flywheel the assumption was made that the fluctuation in shaft speed during a complete cycle should not exceed 10%.

5.6 Belt drive

One shaft is driven by the electric motor via a V-belt while the second shaft is connected to the first by a timing belt. The respective pulleys are keyed to the shafts. Timing belts are positive transmission devices, which means that slipping can not occur. Thus, a constant phase difference between the two pistons can be maintained at all times.

The test-rig is designed to allow the use of various regenerator housings of different lengths. Thus, the distance between the two shafts changes, and the belt drive has to compensate this length while maintaining an adequate tension. In order to provide this compensation (and also to reduce vibrations in the belt due to the relatively large distance of about 1.5 m between the shafts), an idler (Figure 11) was placed in between. This device consists of wheels with flat or toothed profiles guiding the belt. The wheels are carried by needle bearings sitting on pins which can be clamped along vertical slots in order to compensate any change in length of the belt.

In order to maintain an accurate phase difference when the distance between the two shafts needs to be changed, both flywheels can be locked by pins at an angular spacing of 30° around the circumference of the flywheels. Thus, the shaft-assembly can be moved along an aligning slide, clamped to the table, and the belt tension can be readjusted by moving the idler wheels along the vertical slots.

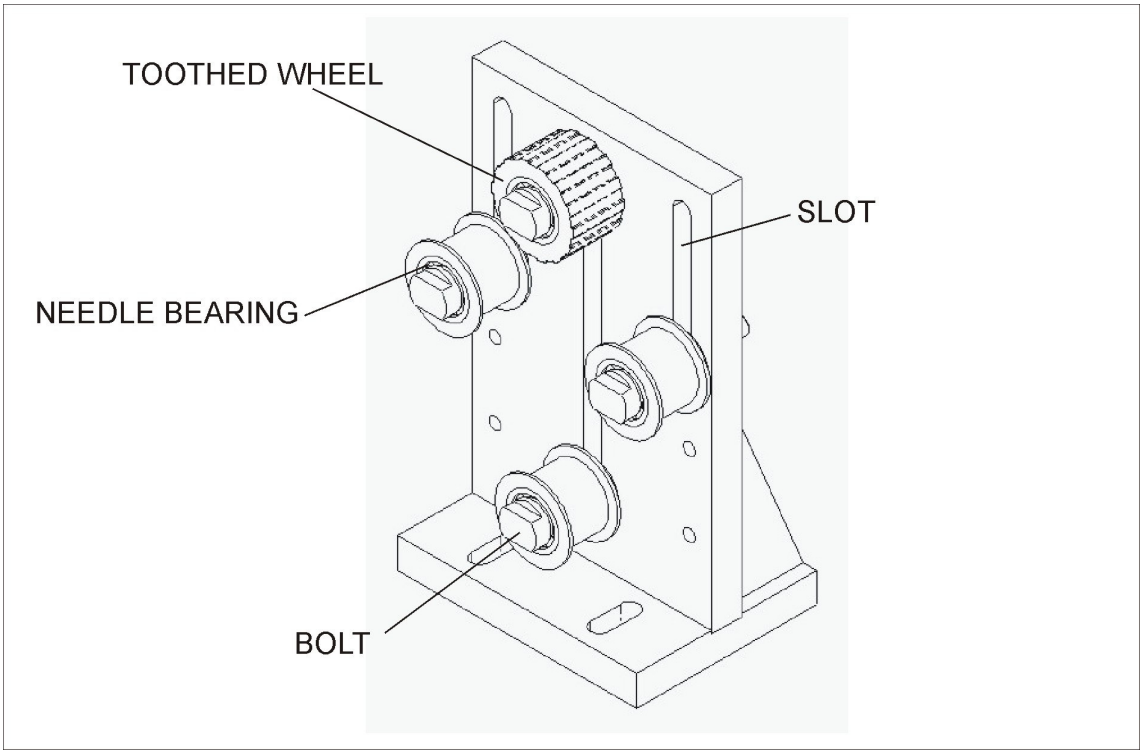

Figure 11: Idler

6. Data acquisition system

For reasons of compatibility a similiar data acquisition system to the DH1 experimental rig was chosen (Figure 12). This included the employment of the same measurement instrumentation and a similiar data acquisition software.

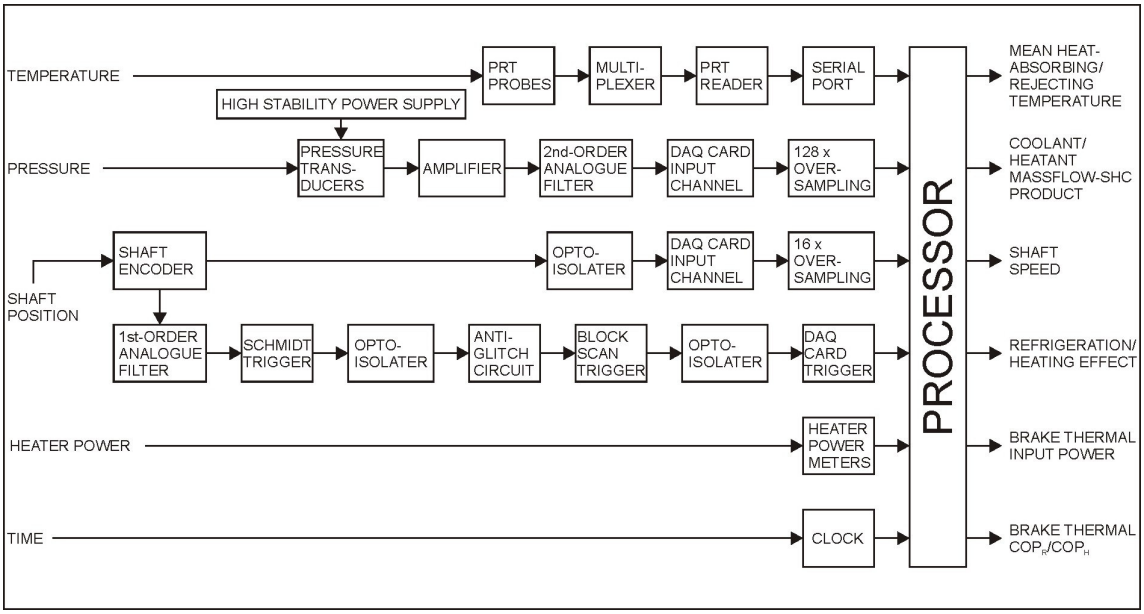

Figure 12: Block diagram of data acquisition system

6.1 Measuring instrumentation

The measurement instrumentation mainly consists of pressure and temperature sensors. The absolute gas pressure is measured on each side of the regenerator (hot and cold side). Temperatures are also measured at the hot and cold end as well as three positions in an axial direction in the regenerator (to detect axial temperature profiles in the matrix). Additionally, the inlet and outlet temperatures of the heatant and coolant fluid are measured in order to determine the absorbed and rejected heat in the heat exchangers. The required massflow-specific-heat-capacity product can be derived from measuring the temperature difference across the heaters in the respective coolant/heatant circuit since the power input is known.

The pressure transducers (Figure 13) are able to measure pressures up to 34.5 bar. The signals pass through the amplifier and are recorded by a data acquisition card in the computer. Measurement of the piston position (and therefore the piston displacement) allows a pV-loop integration in the data acquistion program which then calculates the indicated input power.

Temperature sensors are ceramic-encased platinum RTD elements (embedded in cylindrical stainless steel sheaths for protection). The temperature range is -50°C to 600°C at an accuracy of 0.1% (DIN standard 43760).

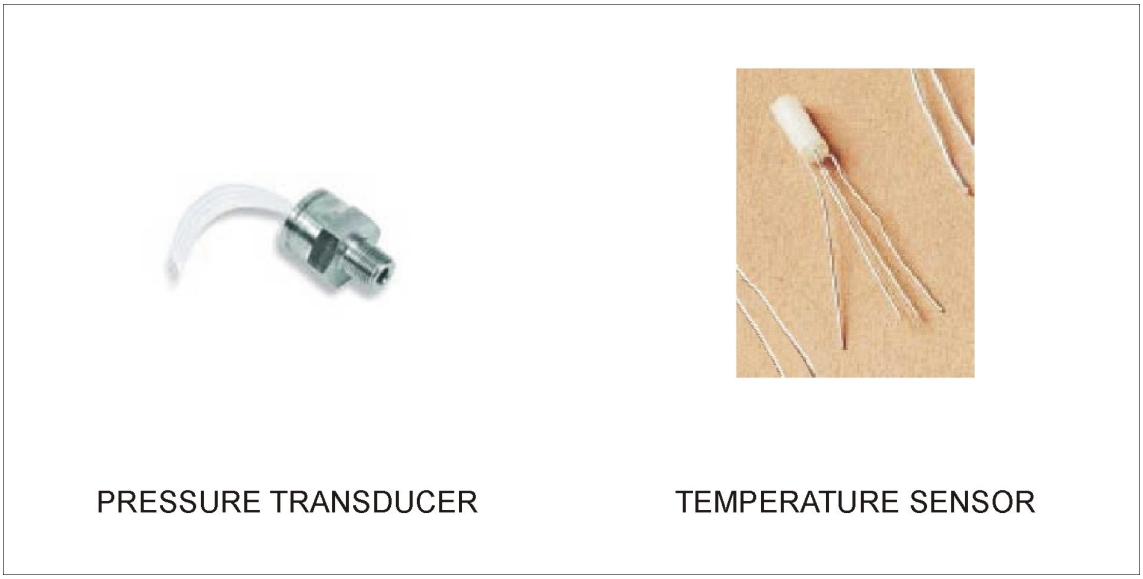

Figure 13: Pressure and temperature sensors

Finally, the shaft speeds are measured by counting the pulses from optical switches triggered by encoder wheels (Figure 14). The angular spacing of the slots is 5°; the pulses also trigger the data acquisition card in the computer. A single hole along the circumference triggers a second optical switch, thus indicating the position of the crank. The relative angular position of this index pulse (with respect to the top dead centre for each shaft) was determined by measuring the piston displacement with an accurate digital feeler gauge.

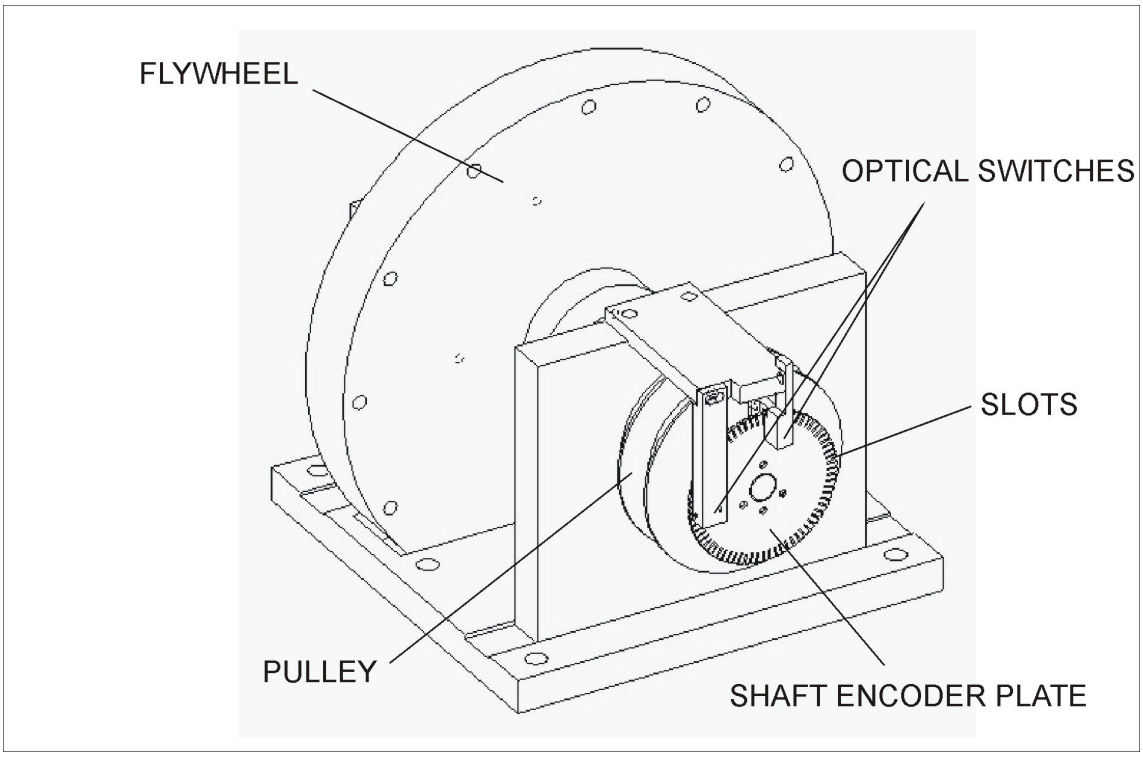

Figure 14: Shaft encoder wheels

6.2 Data acquisition software

The data acquisition software is written in C++ and records the measured values. Figure 15 shows a basic flow diagram of the program. Only a short description is given here; a complete print-out can be found in Appendix B.

After initializing the data acquisition card (and reading the pressure transducer offsets from a file), the main program enters a loop in which the shaft speed and temperatures are repeatedly measured. Before following the data recording path (by pressing *CTRL + D*) the heater input power of the heat absorbing and heat rejecting circuit can be entered. The main routine of the program is carried out by the module DATA_OUT.C. Here, a file name for the stored data can be created before the first temperature data set is taken.

The program now enters a loop in which the oversampling of the pressure measurements takes place. The data acquisition card sends a digital output to the trigger system of one shaft in order to activate it. Thus, every 5° a pulse from the optical switch triggers the card which reads pressure data for 16 revolutions. The DAQ-card then activates the trigger system on the second shaft, and repeats the process. This loop is repeated eight times resulting in 128X-oversampling of the pressure data. Each time a pulse comes from the index optical switch a 5V signal from a battery is superimposed onto the pressure data, thus indicating the angular position of the crank.

Once the pressure oversampling is completed, a final set of temperatures is measured. The start, end, and average values of shaft speed and temperatures are stored in the file.

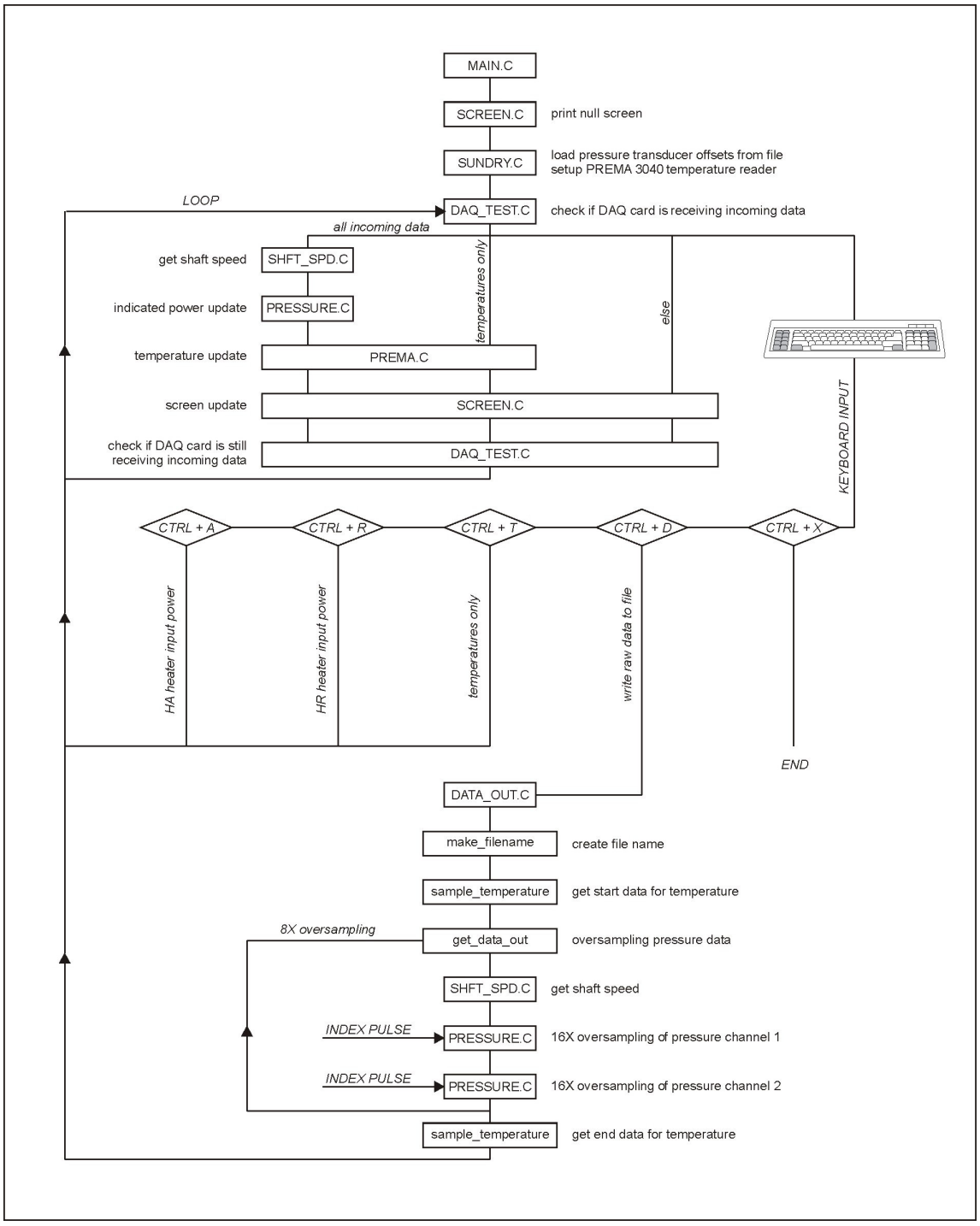

Figure 15: Flow diagram of the data acquisition program

7. Summary

A test-rig has been designed which allows the investigation of various aspects of the regenerator in Stirling-cycle heat-pumps and refrigerators. The set-up was kept as basic as possible, in order to avoid influences stemming from specific configurations. Although the main objective was to investigate various matrix materials, the impact of even more variables on the regenerator behaviour can be examined:

- speed of the cycle
- swept volume
- dead volume
- regenerator volume
- length and diameter of the regenerator matrix
- materials, such as metallic mesh, cotton whool and various synthetic fibres
- package density and fibre / wire diameter of the matrix
- mean pressure
- phase angle
- temperature levels

References

Bartolini, C. M.; Pelagalli, L.: Parametric theoretical analysis of Stirling engine regenerator efficiency.
5th International Stirling Engine Conference 1991 in Dubrovnik, ISEC - 91045, pp. 221 - 219

Benvenuto, G.; De Monte, F.: A simple approach to calculate the regenerator effectiveness in Stirling machines.
7th International Conference on Stirling Cycle Machines 1995 in Tokyo, ICSC - 95046, pp. 307 - 313

Carlson, H.; Kühl, H.-D.; Schulz, S.; Thomas, B.: Effects on an improved hot regenerator on the performance of a Vuilleumier heat pump.
6th International Stirling Engine Conference 1993 in Eindhoven, ISEC - 93052, pp. 233 - 238

Cho, K.-S.; Noh, K.-W.; Kim, S.-T.: Review of unsteady effect on the regenerator effectiveness.
8th International Stirling Engine Conference 1997 in Ancona, ISEC - 97055, pp. 391 - 398

Hamaguchi, K.; Hiratsuka, Y.; Miyabe, H.: Improvement on regenerator matrix properties by the combined mesh wire gauzes.
Proceedings of the 4th International Conference on Stirling Engines 1988, 082, pp. 387 - 392

Hamaguchi, K.; Kaminishizono, T.: Effects of regenerator characteristics on semi-free piston Stirling engine alternator performance.
6th International Stirling Engine Conference 1993 in Eindhoven, ISEC - 93029, pp. 161 - 166

Haywood, D., Raine, J.K., Gschwendtner M.A.: Investigation of seal performance in a 4-a double-acting Stirling cycle heat-pump/refrigerator.
Proceedings of the 10th International Stirling Engine Conference, Osnabrück, 24-28th September 2001, 181-188

Isshiki, H.; Watanabe, H.: A study on optimum design of Stirling engine regenerators.
Proceedings of the 4th International Conference on Stirling Engines 1988, 083, pp. 393 - 397

Kagawa, N.; Ohyama, T.: Regenerator loss of 3 kW Stirling engine.
9th International Stirling Engine Conference 1999 in Pilanesburg, ISEC - 99037, pp. 201 - 206

Kentfield, J. A. C.: The fundamental thermo-fluids of a Stirling engine type regenerator operating at constant volume.
6th International Stirling Engine Conference 1993 in Eindhoven, ISEC - 93041, pp. 197 - 202

Kojiama, H.; Hashimoto, K.; Goto, K.; Sato. T.: A comparative study of regenerator elements for use with a practical Stirling engine.
Proceedings of the 4th International Conference on Stirling Engines 1988, 084, pp. 399 - 402

Kühl, H.-D.; Schulz, S.: A 2nd order regenerator model including flow dispersion and bypass losses.
Proc. 31th IECEC, Washington, USA, 1996, Vol. 2, pp. 1343 - 1348

Kühl, H.-D.; Schulz, S.; Walther, C.: Theoretical models and correlations for the flow friction and heat transfer characteristics of random wire regenerator materials.
Proc. 33th IECEC, Colorado Springs, USA, 1998, #207

Lee, G. T.; Kang, B. H.: Regenerator efficiency enhancement due to the combination of regenerator materials in an oscillating flow of a Stirling cycle machine.
8th International Stirling Engine Conference 1997 in Ancona, ISEC - 97053, pp. 381 - 390

Moriya, S.; Isshiki, N; Kikuchi, S.: Studies on regenerator elemt for internal combustion Stirling engine.
5th International Stirling Engine Conference 1991 in Dubrovnik, ISEC - 91058, pp. 291 - 296

Tanaka, M.; Chisaka, F.: Thermal performance of regenerator.
Proceedings of the 4th International Conference on Stirling Engines 1988, 080, pp. 375 - 380

Tanaka, M.: Effect of wire diameter on regenerator performance.
6th International Stirling Engine Conference 1993 in Eindhoven, ISEC - 93078, pp. 353 - 358

Tanaka, M.; Hamaguchi, K.: The design of Stirling engine regenerator.
7th International Conference on Stirling Cycle Machines 1995 in Tokyo, ICSC - 95049, pp. 329 - 334

Tsuchiya, K.; Nagase, H.; Ohkita, H.; Fujii, I.: A new method for measuring pressure drop in a regenerator matrix under periodic flow condition.
Proceedings of the 4th International Conference on Stirling Engines 1988, 081, pp. 381 - 386

Tsuchiya, K.; Segawa, M.; Fujii, I.: Evaluation of pressure drop in regenerator matrix under periodic flow condition.
5th International Stirling Engine Conference 1991 in Dubrovnik, ISEC - 91075, pp. 393 - 398

Tsuchiya, K.; Uchida, R.; Makino, H.: Pressure drop in heat exchanger element under periodic flow condition.
6th International Stirling Engine Conference 1993 in Eindhoven, ISEC - 93066, pp. 297 - 302

Wei, D.; Fedele, L.; Naso, V.; Walker, G.: Optimal design of packed regenerator of Stirling engine for minimum flow resistance.
8th International Stirling Engine Conference 1997 in Ancona, ISEC - 97080, pp. 579 - 588

Zhiyuan, L.; Hongshuo, L.: Research on a new filler of Regenerator in Stirling engine.
7th International Conference on Stirling Cycle Machines 1995 in Tokyo, ICSC - 95048, pp. 321 - 327